arXiv:cond-mat/0409378v2 [cond-mat.dis-nn] 23 Mar 2005

Geographical threshold graphs with small-world and scale-free properties

Naoki Masuda,[1,2] Hiroyoshi Miwa,[3] and Norio Konno[4]

[1]*Laboratory for Mathematical Neuroscience, RIKEN Brain Science Institute, 2-1, Hirosawa, Wako, Saitama 351-0198, Japan*

[2]*Aihara Complexity Modelling Project, ERATO, JST, 3-23-5, Uehara, Shibuya, Tokyo 151-0064, Japan*

[3]*Department of Informatics, School of Science and Technology, Kwansei Gakuin University, 2-1, Gakuen, Sanda, Hyogo 669-1337, Japan*

[4]*Faculty of Engineering, Yokohama National University, 79-5, Tokiwadai, Hodogaya, Yokohama 240-8501, Japan*

(Dated: Received 15 September 2004)

Abstract

Many real networks are equipped with short diameters, high clustering, and power-law degree distributions. With preferential attachment and network growth, the model by Barabási and Albert simultaneously reproduces these properties, and geographical versions of growing networks have also been analyzed. However, nongrowing networks with intrinsic vertex weights often explain these features more plausibly, since not all networks are really growing. We propose a geographical nongrowing network model with vertex weights. Edges are assumed to form when a pair of vertices are spatially close and/or have large summed weights. Our model generalizes a variety of models as well as the original nongeographical counterpart, such as the unit disk graph, the Boolean model, and the gravity model, which appear in the contexts of percolation, wire communication, mechanical and solid physics, sociology, economy, and marketing. In appropriate configurations, our model produces small-world networks with power-law degree distributions. We also discuss the relation between geography, power laws in networks, and power laws in general quantities serving as vertex weights.

PACS numbers: 89.75.Hc, 89.75.Da, 89.75.Fb

I. INTRODUCTION

Networks of interacting agents such as humans, computers, animal species, proteins, and neurons have been investigated vigorously. They are typically complicated, meaning that their structures are far from absolutely regular or entirely random. Two principal quantities characterizing networks are the average shortest path length L and the clustering coefficient C. The number of edges in the shortest path averaged over all vertex pairs defines L. Most real networks have small L, namely $L \propto \log n$ or even less, where n is the number of vertices. The local clustering coefficient is the normalized number of connected triangles containing a specific vertex. If the vertex degree is k, or there are k edges adjacent to the vertex, the normalization factor is $k(k-1)/2$. This quantity averaged over all the vertices defines C, and real networks usually have large C. A small L and a large C cannot be simultaneously realized either by lattices, trees, or the ordinary random graphs [1, 2]. Then, Watts and Strogatz proposed the small-world networks that fulfill these requirements at the same time [1].

Another important observation is that not all but many real networks have power-law degree distributions $p(k) \propto k^{-\gamma}$, typically with scaling exponent $2 < \gamma < 3$ [2]. The small-world networks are short of the scale-free property. In light of this, Barabási and Albert (BA) proposed a network model that generates scale-free networks with $\gamma = 3$ [2]. Two essential features of the BA model are (i) network growth realized by sequentially adding vertices and edges, and (ii) preferential attachment, meaning that newly introduced edges are more prone to be linked to vertices with larger k. Since the proposal of the BA model, its various extensions and related models, such as the fitness model and the hierarchically growing models, have been presented. These models are successful in incorporating more realistic aspects of networks including tunable γ and large C that the original BA model actually lacks [2, 3, 4, 5, 6, 7, 8, 9].

To sum up, some BA-type models and hierarchical networks own large C, small L, and scale-free $p(k)$. However, real scale-free networks are not necessarily growing. The number of vertices may not change greatly over time for networks of friends, companies, interacting proteins, and neurons, to name a few. In view of this, a class of nongrowing scale-free networks has been studied in which whether edges are created relies on interaction of vertices with intrinsic weights [10]. Weights represent the fitness of vertices to win edges [10, 11,

12] and are interpreted as, for example, capitals, social skills, activity levels, information contents, concentration or mass of physical or chemical substances, and the vertex degree itself. The role of such vertex fitness was argued in growing models as well [3]. To our surprise, scale-free $p(k)$ emerges even from weight distributions devoid of power laws [10, 13, 14, 15]. As a remark, if an edge exists when the sum of two vertices' weights exceeds a prescribed threshold, the network is equivalent to the so-called threshold graph [16]. This case eases analytical treatments.

Our focus in this paper is the geographical extension of the nongrowing scale-free networks, which has been overlooked so far. Actually, real networks are often embedded in topological spaces. Even the Internet, in which the speed of information transmission is technically independent of the physical distance, is subject to geographical constraints because of wiring costs [5, 6, 7, 17]. In addition, it is often advantageous to map nonphysical quantities or networks into geographical spaces by, for example, the principal component analysis. Then, influence of the distance between graduated traits is questioned.

In fact, the Watts-Strogatz small-world network already addressed this issue since it is constructed on lattice substrates [1]. Let us denote by $g(r)$ the probability that two vertices with distance r are connected. In lattice networks supplied with additional edges, where $g(r) \propto r^{-\delta}$, generated networks have small L when δ is smaller than a critical value [18, 19, 20]. Otherwise, global connections are too scarce to elicit the small-world property. The same is true for growing scale-free networks. Although the BA model is irrelevant to embedding spaces, which is actually the main cause for small C, it has been extended to incorporate underlying geographical spaces and $g(r) = r^{-\delta}$. Then, a transition from the scale-free to nonscale-free regime as well as one from small L to large L occurs at a certain δ [4, 5, 6, 7].

Although $g(r)$ plays a key role in determining the network structure, characterization of $g(r)$ in real-world networks still seems controversial. In applications such as the Internet routing [21] and neural networks [22], $g(r)$ decaying exponentially or in a Gaussian manner is commonly used. Exponential decays are also inferred from biological neural networks [23]. However, many other data are in favor of $g(r) \propto r^{-\delta}$. For instance, a recent extensive analysis of the Internet concludes $g(r) \propto r^{-1}$ [6]. Power laws also hold for macroscopic connectivity of brain regions identified by correlated activities [$g(r) \propto r^{-2}$] [24] and for microscopic neural networks [25]. In social sciences, evaluating $g(r)$ seems more difficult

because of presumably larger noises. Accordingly, both power-law and exponential forms of $g(r)$ have been inferred, sometimes even from identical data [26, 27]. In the face of the ambiguity of available data, it is worthwhile to examine models to see how various types of $g(r)$ affect network properties to help interpret real data.

In the context of nongrowing geographical networks, there is an algorithm that generates $p(k) = k^{-\gamma}$ with a prescribed γ [17]. However, investigations of nongrowing geographical networks are largely missing, particularly when interaction of vertices, which is not considered in [17], takes place. We examine a geographical threshold network model with various configurations. In Sec. II, we review the nongeographical threshold model with vertex weights. In Sec. III, we introduce the geographically extended model and analyze some practical cases, including the unit disk graph and the gravity model. Section IV is devoted to discussing our model in the context of network search problems and real data.

II. NONGEOGRAPHICAL THRESHOLD NETWORK MODEL

Before taking geography into account, we briefly summarize the ordinary threshold network model, which constitutes a subclass of networks with intrinsic vertex weights [10, 13, 14, 15].

We prepare n vertices denoted by v_i $(1 \leq i \leq n)$, each of which carries a weight variable $w_i \in \mathbb{R}$ randomly and independently distributed as specified by the density function $f(w)$. As mentioned in Sec. I, w_i quantifies the propensity for v_i to gain edges. Let

$$F(w) = \int_{-\infty}^{w} f(w')dw' \tag{1}$$

be the cumulative distribution function. We explain with additive weights since multiplicative weights are transformed into additive weights by taking the logarithm. In the nongeographical threshold model, an edge exists between v_i and v_j $(i \neq j)$ if and only if $w_i + w_j \geq \theta$. When n is sufficiently large, the weight w uniquely determines the vertex degree k by

$$k \;=\; n\left[1 - F\left(\theta - w\right)\right]. \tag{2}$$

Using Eq. (2), the degree distribution $p(k)$ $(0 \leq k < n)$ is written as

$$\begin{aligned} p(k) &= f(w)\frac{dw}{dk} \\ &= \frac{f\left[\theta - F^{-1}\left(1-\frac{k}{n}\right)\right]}{nf\left[F^{-1}\left(1-\frac{k}{n}\right)\right]}. \end{aligned} \tag{3}$$

Because the model is simple, L, C, and the correlation between the degrees of adjacent vertices can be analytically derived as well [13, 15]. The small-world properties characterized by a large C and a small L are fulfilled for a wide choice of $f(w)$. More microscopically, vertices with small degrees have $C(k)$ near 1 and form the peripheral part of the network. It is connected to the cliquish core with larger k and smaller $C(k)$. Strictly speaking, the core consists of the vertices with $w \geq \theta/2$, and the separability of this kind is known in the graph theory [16]. A similar separability is also mentioned in other literature [11].

The degree distribution depends on $f(w)$. An easily solvable example is the exponential weight distribution given by

$$f(w) = \lambda e^{-\lambda w} \quad (0 \leq w). \tag{4}$$

We set $\theta > 0$ because otherwise the network becomes the complete graph. Although $f(w)$ in Eq. (4) is not reminiscent of the power law, substitution of Eq. (4) into Eq. (3) yields $p(k) \propto k^{-2}$ [10]. It follows that $C(k) \propto k^{-2}$ and $\overline{k}(k) \propto k^{-1}$, where $\overline{k}(k)$ is a measure of degree correlation, namely, the average degree of the neighbors of a reference vertex with degree k [13, 15]. The same scaling law is also maintained for the logistic distribution $f(w) = \beta e^{-\beta w}/\left(1+e^{-\beta w}\right)^2$, which is just a slight modification of Eq. (4) [15]. Another major class of $f(w)$ is the Pareto distribution defined by

$$f(w) = \frac{a}{w_0}\left(\frac{w_0}{w}\right)^{a+1} \quad (w \geq w_0), \tag{5}$$

where $a, w_0 > 0$. Equation (5) leads to $p(k) \propto k^{-\gamma}$ with $\gamma = (a+1)/a > 1$, $C(k) \propto k^{-1}$, and $\overline{k}(k) \propto k^{-1}$ [15]. Particularly, $C(k) \propto k^{-1}$ is more consistent with real data [8] compared with $C(k) \propto k^{-2}$ derived from Eq. (4). The asymptotics is the same for the Cauchy distribution $f(w) = 1/[\pi(1+w^2)]$ $(w \in \mathbb{R})$, which is devoid of the lower bound of w. The inverse problem to determine $f(w)$ from $p(k)$ has also been addressed [14].

A crux of the threshold model is that scale-free $p(k)$ results from a wide class of $f(w)$. Analytical and numerical evidence indicates that $\gamma = 2$ is the baseline scaling exponent of

the threshold model, which contrasts with $\gamma = 3$ for the BA model [15]. Since the effect of a lower bound of w seems marginal, we mainly use the exponential and Pareto distributions for the geographically extended model.

III. GEOGRAPHICAL THRESHOLD NETWORK MODEL

To generalize the model introduced in Sec. II in the geographical case, we assume that vertices are uniformly and independently distributed with density ρ in a d-dimensional Euclidean space whose coordinates are denoted by x_1, x_2, ..., x_d. Then a pair of vertices with weights w, w', and Euclidean distance r are connected if and only if

$$(w + w')h(r) \geq \theta, \tag{6}$$

where $h(r)$ is assumed to decrease in r, although $h(r)$ increasing in r has also been considered in other models [4, 7, 18]. As a special case, Eq. (6) with $h(r) \propto r^{-1}$ is equivalent to the Boolean model [28].

Based on Eq. (6), two vertices with weights w and w' are adjacent if

$$r \leq h^{-1}\left(\frac{\theta}{w + w'}\right). \tag{7}$$

For a vertex with weight w, the degree k is represented by

$$k = \int f(w')\, dw' \left[\text{number of vertices in a ball of radius } = h^{-1}\left(\frac{\theta}{w + w'}\right)\right]. \tag{8}$$

This recovers a general formulation [10, 13], in which k is calculated from the joint probability as a function of w and w' that a pair of vertices are connected. Combination of Eq. (8) and $f(w)$ provides $p(k)$. If we take an average over w but not over r, we obtain $g(r)$. Although $g(r)$ decreases in r if $h(r)$ does, it generally differs from $h(r)$.

A. Unit disk graph

If $f(w) = \delta(w_0)$, where δ is the delta function, two vertices are adjacent when $2w_0h(r) \geq \theta$. Since $h(r)$ decreases in r, this condition is equivalent to $r \leq r_0$ where $2w_0h(r_0) = \theta$. Accordingly,

$$g(r) = \begin{cases} 1 & (r \leq r_0), \\ 0 & (r > r_0), \end{cases} \tag{9}$$

and the generated network is the unit disk graph, which is applied to modeling broadcast and sensor networks [16, 29]. If $f(w)$ has a finite support, the network resembles the unit disk graph in the sense that there exists an upper limit $r = r_0$ only below which $g(r) > 0$. With this case included, long-range edges are entirely prevented, and the network has $L \propto n^{1/d}$, spoiling the small-world property. However, if we allow $g(r) = p$ $(r > r_0)$ with $0 < p \cong n^{-1} \ll 1$, we have a type of the Watts-Strogatz small-world networks with small L [2]. Even so, $p(k)$ is essentially homogeneous. To introduce the scale-free property, we need to use more inhomogeneous vertex weights.

B. Exponential weight distribution with $h(r) \propto r^{-\beta}$

Let us consider the exponential weight distribution given in Eq. (4) and set

$$h(r) = r^{-\beta}, \tag{10}$$

where $\beta \geq 0$. This case generalizes the nongeographical model explained in Sec. II, which corresponds to $\beta = 0$. For a larger β, geographical effects are more manifested. As a function of the weight, the degree is calculated as follows:

$$\begin{aligned} k(w) &= \int_0^\infty f(w')dw' \int_{(w+w')/r^\beta \geq \theta} \rho \, dx_1 \dots dx_d \\ &= \rho \int_0^\infty \lambda e^{-\lambda w'} \pi^{d/2} \Gamma\left(\frac{d}{2}+1\right) \left(\frac{w+w'}{\theta}\right)^{d/\beta} dw' \\ &= c_1 e^{\lambda w} \Gamma\left(\frac{d}{\beta}+1, \lambda w\right), \end{aligned} \tag{11}$$

where

$$\Gamma(\alpha, x) \equiv \int_x^\infty t^{\alpha-1} e^{-t} dt. \tag{12}$$

is the incomplete Gamma function,

$$c_1 \equiv \frac{\rho \pi^{d/2}}{(\theta\lambda)^{d/\beta}} \Gamma\left(\frac{d}{2}+1\right), \tag{13}$$

and $\Gamma(\alpha) \equiv \Gamma(\alpha, 0)$ is the ordinary Gamma function. To obtain $p(k)$ from $k(w)$, we just need to eliminate w from Eq. (11) as we have done in Eq. (3).

However, an analytical form of $p(k)$ corresponding to Eq. (11) is unavailable due to the incomplete Gamma function. Accordingly, let us deal with some special cases. By

integrating Eq. (12) by parts, we derive

$$\Gamma(\alpha, x) = (\alpha - 1)!\, e^{-x} \sum_{\alpha'=0}^{\alpha-1} \frac{x^{\alpha'}}{\alpha'!} \quad (\alpha \in \mathbb{Z}), \tag{14}$$

where $\mathbb{Z}$ is the set of integers. In the limit $\beta \to 0$, Eq. (14) implies

$$\lim_{\beta \to 0} \frac{\Gamma\left(\frac{d}{\beta} + 1, \lambda w\right)}{\left(\frac{d}{\beta}\right)!} = 1. \tag{15}$$

Actually, k explodes as $\beta \to 0$ because Eq. (15) means $\lim_{\beta \to 0} \Gamma\left((d/\beta) + 1, \lambda w\right) = \infty$, reflecting the density notation of the vertex distribution. Putting aside this nonessential point, $\Gamma\left((d/\beta) + 1, \lambda w\right)$ is asymptotically independent of w, and we have

$$k(w) \propto e^{\lambda w} \tag{16}$$

and

$$p(k) \propto e^{-2\lambda w} \propto k^{-2}, \tag{17}$$

which reproduces the results for the nongeographical counterpart [10, 13, 15]. For a sufficiently small β, Eq. (15) effectively approximates the incomplete Gamma function. Consequently, scale-free $p(k)$ with $\gamma = 2$ or a slightly larger γ is almost preserved.

When $\beta = d$, we obtain

$$k(w) = c_1 e^{\lambda w} \Gamma\left(2, \lambda w\right) = c_1(1 + \lambda w) \tag{18}$$

and

$$p(k) = \frac{\lambda e^{-\lambda w}}{c_1 \lambda} = \frac{\exp\left(1 - \frac{k}{c_1}\right)}{c_1}. \tag{19}$$

The degree distribution now has an exponential tail, and hubs are less likely compared with Eq. (17). Another special case with $\beta = d/2$ leads to

$$k(w) = c_1 \left(2 + 2\lambda w + \lambda^2 w^2\right) \tag{20}$$

and

$$p(k) = \frac{\lambda e^{-\lambda w}}{2c_1(\lambda + \lambda^2 w)} = \frac{\exp\left(1 - \sqrt{\frac{k}{c_1} - 1}\right)}{2c_1^{3/2}\sqrt{k - c_1}}. \tag{21}$$

Equation (21) is a stretched exponential distribution with a minor modification factor $k^{-1/2}$, and $p(k)$ decays more slowly than in Eq. (19) naturally because $\beta = d/2 < d$.

Similarly, k and w are connected by a power law relation if $\beta > 0$. Then, $p(k)$ is a type of stretched exponential. In geographical preferential attachment models, the crossover from a power-law tail to a stretched exponential tail occurs at a finite value of the control parameter similar to β [4, 5, 6, 7]. We could say that, in our model, the same transition happens at $\beta = 0$. However, the gist is that for a sufficiently small β, $p(k)$ is practically indiscernible from the scale-free distribution.

Since it seems difficult to analytically calculate other network characteristics such as L and C, we resort to numerics. We uniformly scatter $n = 10000$ vertices in a two-dimensional square lattice with side length 100 and periodic boundary conditions. Because more edges obviously means smaller L, the mean degree denoted by $\langle k \rangle$ is kept at 20. The analytic expression for $\langle k \rangle$ is available only when $\beta = 0$ as follows [13, 15]:

$$\langle k \rangle = e^{-\lambda\theta} \left(\rho l^d + \lambda\theta \right), \tag{22}$$

where l is the side length of the area. Therefore, we manually modulate θ to preserve $\langle k \rangle$ as we vary β. Excluding isolated components, which actually consist of just a few vertices, we show a dependence of L and C on β in Figs. 1(a) and 1(b), respectively. Although the main simulations are done with $n = 10000$ (thickest lines), we also show results for $n = 2000$ (thinnest lines), 4000, 6000, and 8000. The inset of Fig. 1(a) shows the dependence of L on n, with upper lines corresponding to larger values of β. Figure 1(a) shows that L is insensitive to n only when $\beta < 0.5$. We expect that $L \propto \log n$ approximately holds in this regime. On the other hand, we expect $L \propto n^{1/d}$ or similar scaling for larger β. As β increases, C decrease to some extent but not too much to spoil the clustering property [Fig. 1(b)]. Figures 1(c), 1(d), and 1(e) show $p(k)$ (crosses) and $C(k)$ (circles) for $\beta = 0.5$, $\beta = 1.5$, and $\beta = 2.5$, respectively. As expected, small β yields a long tail indicative of the power law [Fig. 1(c)]. In contrast, Fig. 1(e) shows that $p(k)$ decays much faster when β is larger. Consequently, networks generated by sufficiently small β are endowed with the scale-free and small-world properties simultaneously in a geographical context, which extrapolates the nongeographical results with $\beta = 0$. In regard to the vertex-wise clustering coefficients, $C(k) \propto k^{-2}$ holds when $\beta = 0$ [13, 15]. The numerical results in Figs. 1(c), 1(d), and 1(e) (circles) support $C(k) \propto k^{-2}$ except that vertices with small $C(k)$ are more scarce for larger β.

The probability $g(r)$ that two vertices with distance r are adjacent becomes

$$\begin{aligned} g(r) &= \int_0^\infty \lambda e^{-\lambda w} dw \int_{(w+w')/r^\beta \geq \theta} \lambda e^{-\lambda w'} dw' \\ &= \int_0^{\theta r^\beta} \lambda e^{-\lambda w} dw \int_{\theta r^\beta - w}^\infty \lambda e^{-\lambda w'} dw' + \int_{\theta r^\beta}^\infty \lambda e^{-\lambda w} dw \\ &= e^{-\lambda \theta r^\beta} (\lambda \theta r^\beta + 1), \end{aligned} \tag{23}$$

indicating a stretched exponential decay in r unless $\beta = 0$. Particularly, the main decay rates for $\beta = 1$ and $\beta = 2$, respectively, correspond to the standard exponential and the Gaussian, which are widely used in applications [21, 22]. As a general remark, $g(r)$ does not coincide with $h(r) \propto r^{-\beta}$ even asymptotically.

The loss of the small-world property for large β seems to stem from the (stretched) exponential decay of $g(r)$. In addition, $g(r)$ derived here qualitatively disagrees with many real data [6, 24, 25]. As a result, exponential types of $g(r)$ and the Gaussian $g(r)$ may be far from universal. This is a striking caveat to many fields, such as neuroscience, social dynamics, and epidemics, which conventionally assume geographical networks with exponentially decaying or Gaussian $g(r)$. We do not explore consequences of $h(r)$ that decays faster than $h(r) \propto r^{-\beta}$, since such an $h(r)$ must yield even larger L. On the other hand, $h(r)$ with slower decays, or $h(r) \propto (\log r)^{-1}$, is examined in Sec. III D.

C. Power-law weight distribution with $h(r) \propto r^{-\beta}$

Quantities that can serve as vertex weights, such as the city and firm sizes [30, 31, 32, 33], number of pages in a website [34], land prices [35], incomes [36], importance of airports [9], and importance of academic authors [9], are often distributed according to power laws. The history of these power laws is much longer, dating back to the Pareto and Zipf laws, than those recently found for networks [2]. The simplest way to associate the power laws of networks with those of vertex weights is simply to interpret the vertex degree as the weight. However, w and k are generally nonidentical [9, 15].

Let $f(w)$ be the Pareto distribution given in Eq. (5). With the interaction strength

decaying algebraically [Eq. (10)], we have

$$\begin{aligned} k(w) &= \rho \int_{w_0}^{\infty} \frac{a}{w_0} \left(\frac{w_0}{w'}\right)^{a+1} \pi^{d/2} \Gamma\left(\frac{d}{2}+1\right) \left(\frac{w+w'}{\theta}\right)^{d/\beta} dw' \\ &= \frac{a w_0^a \rho \pi^{d/2}}{\theta^{d/\beta}} \Gamma\left(\frac{d}{2}+1\right) w^{(d/\beta)-a} \int_{w_0/w}^{\infty} \frac{(1+x)^{d/\beta}}{x^{a+1}} dx \quad (w \geq w_0). \end{aligned} \tag{24}$$

Convergence of $k(w)$ necessitates $-a + d/\beta < 0$. In the limit $w \to \infty$, it holds that

$$\int_{w_0/w}^{\infty} \frac{(1+x)^{d/\beta}}{x^{a+1}} dx \propto \int_{w_0/w}^{\infty} \frac{1}{x^{a+1}} dx \propto \left(\frac{w}{w_0}\right)^a. \tag{25}$$

Therefore,

$$k(w) \propto w^{d/\beta} \tag{26}$$

and

$$p(k) \propto \frac{\frac{a}{w_0}\left(\frac{w_0}{w}\right)^{a+1}}{\frac{d}{\beta} w^{(d/\beta)-1}} \propto k^{-1-(a\beta/d)}. \tag{27}$$

In contrast to the stretched exponential scenario clarified in Sec. III B, the power-law weight distribution produces scale-free $p(k) = k^{-\gamma}$ with $\gamma = 1 + (a\beta/d)$.

For r large enough to satisfy $\theta r^\beta \geq 2w_0$,

$$\begin{aligned} g(r) &= \int_{\theta r^\beta - w_0}^{\infty} \frac{a}{w_0} \left(\frac{w_0}{w'}\right)^{a+1} dw' + \int_{w_0}^{\theta r^\beta - w_0} \frac{a}{w_0} \left(\frac{w_0}{w'}\right)^{a+1} \left(\frac{w_0}{\theta r^\beta - w'}\right)^a dw' \\ &= \left(\frac{w_0}{\theta r^\beta - w_0}\right)^a + \int_1^{b-1} x^{-a-1}(b-x)^{-a} dx, \end{aligned} \tag{28}$$

where $b \equiv \theta r^\beta / w_0$. To show that the integral in Eq. (28) tends to be proportional to $r^{-a\beta}$ as $r \to \infty$, let us evaluate $b^a \int_1^{b-1} A(x) dx$, where $A(x) \equiv x^{-a-1}(b-x)^{-a}$. First, we obtain

$$\begin{aligned} \liminf_{b\to\infty} b^a \int_1^{b-1} A(x) dx &\geq \lim_{b\to\infty} \left(\frac{b}{b-1}\right)^a \int_1^{b-1} x^{-a-1} dx \\ &= \frac{1}{a} \lim_{b\to\infty} \left[1 - (b-1)^{-a}\right] = \frac{1}{a}. \end{aligned} \tag{29}$$

To bound the integral from the above in the limit $b \to \infty$, let us assume $b > 4$. Noting that

$A(x)$ takes the minimum at $x = (a+1)b/(2a+1)$ and that $d^2A(x)/dx^2 > 0$, we derive

$$\begin{aligned}
&\limsup_{b\to\infty} b^a \int_1^{b-1} A(x)dx \\
&\le \lim_{b\to\infty} \left\{ \int_1^{(b+2)/3} \left[\frac{3b}{2(b-1)}\right]^a x^{-a-1}dx + \frac{b^a}{2}\left[A\left(\frac{b+2}{3}\right) + A\left(\frac{(a+1)b}{2a+1}\right)\right]\left[\frac{(a+1)b}{2a+1} - \frac{b+2}{3}\right] \right. \\
&\quad \left. + \frac{b^a}{2}\left[A\left(\frac{(a+1)b}{2a+1}\right) + A\left(b-1\right)\right]\left[(b-1) - \frac{(a+1)b}{2a+1}\right] \right\} \\
&= \lim_{b\to\infty} \left\{ \left[\frac{3b}{2(b-1)}\right]^a \frac{1}{a}\left[1 - \left(\frac{3}{b+2}\right)^a\right] \right. \\
&\quad \left. + \frac{1}{2}\left(\frac{b}{b-1}\right)^a \left[\frac{ab-2a-1}{(2a+1)(b-1)}\right] + O\left(b^{-a}\right) \right\} \\
&= \frac{1}{a}\left(\frac{3}{2}\right)^a + \frac{a}{2(2a+1)} < \infty. \qquad (30)
\end{aligned}$$

Equations (29) and (30) allow us to conclude an algebraic decay $g(r) \propto r^{-a\beta}$ in contrast to Eq. (23). Discussion on network structure is postponed to Sec. III D, where we analyze the gravity model, which ends up with the same asymptotic behavior of $p(k)$ and $g(r)$.

D. Gravity model with Pareto $f(w)$

As shown in Sec. III B, given the exponentially distributed w, $h(r) \propto r^{-\beta}$ with a sufficiently small β yields more or less desired network properties. More rapidly decaying $h(r)$ makes $g(r)$ decrease too fast to elicit small L. How about $h(r)$ that decays more slowly? To address this issue, we apply $h(r) \propto (\log r)^{-1}$. Since $\log r$ can be negative, let us rewrite Eq. (6) as

$$w + w' \ge \theta \log r. \qquad (31)$$

Equation (31) is equivalent to

$$e^w e^{w'} \ge r^\theta. \qquad (32)$$

Since edge formation is suppressed by increasing either β or θ, let us reinterpret θ in Eq. (32) as β, which does not essentially change the model. Further rescaling of the parameters by $W \equiv e^w$, $W \equiv e^{w'}$, and $R = \theta^{-1/\beta} r$ transforms Eq. (32) into

$$\frac{WW'}{R^\beta} \ge \theta. \qquad (33)$$

This is the gravity model often used in physics, sociology, economics, and marketing [26, 30, 37, 38, 39]. The gravity model is suitable in describing interaction of particles in geographical

spaces when the physical gravity ($\beta = 2$) or similar mass interaction based on, for example, populations or chemical substances, is active. In the sociological context, the original model stipulates $\beta = 1$ [30], but β ranging from 0.2 to 2.7 have been inferred from later real data [26, 27, 37, 38, 39, 40].

The original gravity model is geographical but neglects weight distributions. On the other hand, multiplicatively interacting weights with power-law $f(w)$ are used to generate solvable scale-free networks, but they ignore geography [11]. We are interested in combined effects of geography and dispersed vertex weights. The transformation from Eq. (31) to Eq. (33) also rescales $f(w)$ unless it is the delta function. When the weights in Eq. (31) follows the exponential distribution given in Eq. (4), the density $\overline{f}(W)$ of the weights in Eq. (33) becomes

$$\overline{f}(W) = f(w)\frac{dw}{dW} = \lambda \left(\frac{1}{W}\right)^{\lambda+1}, \tag{34}$$

namely the Pareto distribution with $a = \lambda$ and $w_0 = 1$. Although we have started with $h(r) \propto (\log r)^{-1}$ and additive weights, we switch to the gravity-model notation for convenience. Now we rewrite Eq. (33) as

$$\frac{ww'}{r^\beta} \geq \theta \tag{35}$$

and investigate the network structure when $f(w)$ is the Pareto distribution.

Before moving on to the Pareto $f(w)$, let us note that $f(w)$ with a finite support only allows local interaction, as explained in Sec. III A. Then the gravity model yields $L \propto n^{1/d}$, which is realized by atomic and molecular interaction by centrifugal or electric forces; they practically interact only with others nearby. With the Pareto $f(w)$, which facilitates more global interaction, we obtain

$$\begin{aligned} k(w) &= \rho \int_{w_0}^{\infty} \frac{a}{w_0} \left(\frac{w_0}{w'}\right)^{a+1} \pi^{d/2}\Gamma\left(\frac{d}{2}+1\right) \left(\frac{ww'}{\theta}\right)^{d/\beta} dw' \\ &= c_2\, w^{d/\beta}, \end{aligned} \tag{36}$$

where

$$c_2 = \frac{\rho\pi^{d/2}}{\theta^{d/\beta}} \frac{a}{a-\frac{d}{\beta}} w_0^{d/\beta}\, \Gamma\left(\frac{d}{2}+1\right). \tag{37}$$

Equation (36) is essentially the same as Eq. (24), and $\beta > d/a$ must be satisfied for $c_2 > 0$. The original gravity model for social interaction has $\beta = 1$ and $d = 2$ [30], and hence $a > 2$

is necessary. Combination of Eqs. (5) and (36) yields

$$p(k) = \frac{a\beta w_0^a}{c_2 d} w^{-a-(d/\beta)} = \frac{a\beta c_2^{a\beta/d} w_0^a}{d} k^{-1-(a\beta/d)}. \tag{38}$$

When $r^\beta > w_0^2/\theta$, we obtain

$$\begin{aligned} g(r) &= \int_{w_0}^{\theta r^\beta/w_0} \frac{a}{w_0} \left(\frac{w_0}{w}\right)^{a+1} \left(\frac{w w_0}{\theta r^\beta}\right)^a dw + \int_{\theta r^\beta/w_0}^{\infty} \frac{a}{w_0} \left(\frac{w_0}{w}\right)^{a+1} dw \\ &= \frac{w_0^{2a}}{\theta^a} \left(a \log \frac{\theta r^\beta}{w_0^2} + 1\right) r^{-a\beta}. \end{aligned} \tag{39}$$

Comparison of Eqs. (27) and (28) with Eqs. (38) and (39) reveals that the asymptotic behavior of $p(k)$ and that of $g(r)$ coincide with those of the additive weight model with the Pareto $f(w)$ and $h(r) = r^{-\beta}$. Given the Pareto $f(w)$ and $h(r) = r^{-\beta}$, whether multiplicative or additive interaction is used does not matter so much.

Numerically evaluated L, C, $p(k)$, and $C(k)$ for varying β are shown in Fig. 2. We set $n = 10000$, $a = 1$, $w_0 = 1$, and

$$\langle k \rangle = \int_{c_2 w_0^{d/\beta}}^{\infty} k\, p(k)\, dk = \frac{a\beta c_2 w_0^{d/\beta}}{a\beta - d} \tag{40}$$

constant at 20. Figures 2(a) and 2(b) show that L and C have a similar dependence on β to the additive weight model with exponential $f(w)$ [Figs. 1(a) and 1(b)]. Figure 2(a) indicates that a transition from a small-L regime to a large-L regime occurs somewhere around $\beta = 3$. Since Fig. 2(b) supports that C remains finite for large n irrespective of β, the small-world property is suggested for small β. The transition appears similar to the phase transition in geographical BA models [4, 5]. However, in those models, γ does not change in $\beta > 0$ as far as the network is in the small-world regime, whereas it does change here (but see [17]). As shown in Figs. 2(c), 2(d), and 2(e), $p(k)$ (crosses) obey power laws whose scaling exponents are well predicted by Eq. (38) (lines). Consequently, the weighted gravity model realizes scale-free small-world networks when β is small enough. In this scheme, γ is tunable by varying a, β, and d. Circles in Figs. 2(c), 2(d), and 2(e) indicate $C(k) \propto k^{-\gamma'}$ with $\gamma' \cong 2$ or somewhat smaller. Finally, numerically obtained $g(r)$ shown by circles in Figs. 3(a) ($\beta = 2$) and 3(b) ($\beta = 3$) decays algebraically as predicted by Eq. (39).

A generated network is shown in Fig. 4 for $n = 100$, $d = 1$, $a = 1$, $w_0 = 1$, $\beta = 1$, and hence $\gamma = 2$. For demonstration purposes, the vertices are aligned on a one-dimensional ring. In spite of the small size, the figure is indicative of the scale-free and small-world

properties. It is visually comparable to the BA-type scale-free small-world networks on a ring [5] and the Watts-Strogatz non-scale-free small-world networks [1].

In other geographical network models, L becomes large if $g(r)$ decays faster than $g(r) \propto r^{-\delta}$ with a certain $\delta > 0$. For example, a nonscale-free weightless network model on a lattice owns an ultrasmall $L = O(1)$ for $\delta \leq d$, small $L = O(\log n)$ for $d < \delta < 2d$, and large $L = O(n^{1/d})$ for $\delta \geq 2d$ [19]. In another nonscale-free network, $\delta = d + 1$ divides the small-world and large-world regimes [18]. Also in a one-dimensional geographical scale-free network model with preferential attachment, a similar phase transition occurs at $\delta = 1$ [5, 7]. Based on Figs. 1(a) and 2(a), we anticipate that the gravity model has the phase transition at a critical value δ under which the network is geographical, scale-free, and small-world at the same time. We do not examine $h(r)$ decaying faster than $(\log r)^{-1}$ in the additive weight notation [Eq. (31)] or equivalently $h(r)$ decaying faster than algebraically in the multiplicative weight notation [Eq. (35)], for which we expect too large L. Let us mention that $h(r) \propto (\log r)^{-1}$, which other models have largely neglected, may be appropriate if weight interaction is effectively additive.

The results in Sec. III C and those in this section can be captured as a spatial extension of the results in [14], which addresses the inverse problem to determine $f(w)$ from $p(k)$. To obtain $p(k) \propto k^{-\gamma}$, a pair of vertices with weights w and w' that follow $f(w) = \lambda e^{-\lambda w}$ with $\lambda = 1$ are connected with probability proportional to $\exp\left[-(w + w')/(-\gamma + 1)\right]$ [14]. In the gravity model, we have defined $W = \exp(w)$ and $W' = \exp(w')$ so that W and W' follow the Pareto distribution. The probability that the two vertices are connected is proportional to the volume of a d-dimensional ball with radius r_0, where $WW'/r_0^\beta = \theta$. This probability is proportional to $r_0^d \propto (WW'/\theta)^{d/\beta} \propto \exp[(w + w')d/\beta]$. We should have $d/\beta = 1/(\gamma - 1)$, which is consistent with Eq. (38) since $a = \lambda = 1$.

E. Gravity model with exponential $f(w)$

Let us treat the gravity model with the exponential weight distribution. This configuration is equivalent to the model with additive weight interaction, $h(r) \propto (\log r)^{-1}$, and a weight distribution less broad than the exponential distribution. It follows that

$$k(w) = \rho \int_0^\infty \lambda e^{-\lambda w'} \pi^{d/2} \Gamma\left(\frac{d}{2} + 1\right) \left(\frac{ww'}{\theta}\right)^{d/\beta} dw' = c_1 \Gamma\left(\frac{d}{2} + 1\right) w^{d/\beta} \tag{41}$$

and

$$p(k) = \frac{\beta\lambda}{dk^{1-\beta/d}\left[c_1\Gamma\left(d/\beta+1\right)\right]^{\beta/d}} \exp\left[-\lambda\left(\frac{k}{c_1\Gamma\left(d/\beta+1\right)}\right)^{\beta/d}\right], \tag{42}$$

which is a stretched exponential with a modifying factor $k^{-1+\beta/d}$. Furthermore, we have

$$\begin{aligned} g(r) &= \int_0^\infty \lambda e^{-\lambda w} e^{-\lambda\theta r^\beta/w} dw = 4\lambda^2 \int_0^\infty \frac{\cos(\sqrt{\theta r^\beta}u)}{(u^2+4\lambda^2)^{3/2}} du \\ &= 4\lambda^2 \int_1^\infty \frac{e^{-2\lambda\sqrt{\theta r^\beta}t}}{\sqrt{t^2-1}} dt = 4\lambda^2 K_0(2\lambda\sqrt{\theta r^\beta}), \end{aligned} \tag{43}$$

where $K_0(x)$ is the modified Bessel function of the second kind [41, pp.185, 187–188, and 206]. Since $K_0(x)$ tends to

$$K_0(x) = \sqrt{\frac{\pi}{2x}} e^{-x}\left[1 - \frac{1}{8x} + O\left(\frac{1}{x^2}\right)\right] \tag{44}$$

as $x \to \infty$ [41, p.202], Eq. (43) asymptotically behaves as

$$g(r) \cong 2\pi^{1/2}\lambda^{3/2}\left(\theta r^\beta\right)^{-1/4} e^{-2\lambda\sqrt{\theta r^\beta}} \quad (r \to \infty). \tag{45}$$

With the arguments in Sec. III D taken into account, Eq. (45) implies that $g(r)$ decays too fast to make the network small-world. A lesson is that $f(w)$ considerably influences network properties, which is not the case for the nongeographical counterpart [15]. Particularly, the Pareto $f(w)$ can yield scale-free $p(k)$ and the small-world properties, regardless of whether weight interaction is additive or multiplicative. On the other hand, the exponential $f(w)$ explored in this section and Sec. III B induces exponential types of $p(k)$ and large L.

IV. SCALE-FREE NETWORKS AND SCALE-FREE WEIGHT DISTRIBUTIONS

Among the configurations considered in Sec. III, the additive weight model and the gravity model with scale-free $f(w)$ and scale-free $h(r)$ generate small-world networks with scale-free $p(k)$. In this regime, our model relates scale-free $p(k)$, which is of recent research interest, to general power law distributions in nature that have a long history tracing back to Pareto. Let us discuss the relevance of our model to real data.

There is a body of evidence that quantities potentially serving as vertex weights are distributed according to power laws $f(w) \propto w^{-a-1}$. For example, the celebrated Pareto and Zipf laws dictate that incomes and city sizes follow power laws with $a+1 = 2.0$ [30, 31]. More recent data analyses confirm power laws in countrywise city sizes ($a+1 = 1.81$–2.96

with mean $a+1=2.136$) [32], firm sizes ($a+1=2$) [33], the number of pages per website ($a+1=1.65$–1.91) [34], land prices ($a+1=2.1$–2.76) [35], incomes ($a+1=1.7$–2.4) [36], and importance of airports ($a+1=1.67$) [9], to name a few. On the other hand, the original gravity model disregarding weight distributions assumes $\beta=1$ and $d=2$ [30]. Application of the values of a mentioned above to the weighted gravity model yields $\gamma=1+a\beta/d=1.32$–1.98, which is too small to fit real network data whose γ mostly falls between 2 and 3 [2]. As another indication, an extensive data analysis of the Internet revealed $g(r)\propto r^{-\delta}$ with $\delta=1$ [6]. If our model could underlie the Internet, it should mean $a\beta=\delta=1$, and hence $\gamma=1+a\beta/d=3/2$ since $d=2$. This γ is again too small for the real Internet and related computer networks that have $\gamma=1.9$–2.8 [2].

However, we regard that our model is not necessarily implausible. First, our model and also the nonspatial threshold model do not aim to describe growing networks; the Internet is a typical example of growing networks [2]. Our goal is rather to discuss nongrowing networks in a geographical context. As a supporting example, connectivity networks of brain regions have $\gamma=2$, $\delta=a\beta\cong 2$, and $d=2$ [24], which are roughly consistent with Eq. (38). Actually, the brain network does not grow so much once an animal is born.

Second, estimation of β involves much fluctuation because of the difficulty in data acquisition. Since the proposal of the gravity model in which $\beta=1$ was inferred from railway and highway travel data [30], analyses of various social activity data have offered a wide range of β. Among them are investigations of air travels ($\beta=0.2$–2.0) [26, 37, 38], journey to work ($\beta=0.5$–1.2) [27], migration ($\beta=1.59, 2.49$) [39], cedar rapids direct contacts ($\beta=2.74$) [39], marriage ($\beta=0.59, 1.53, 1.59$) [39], and memorizable social interaction ($\beta=2$) [40]. The ambiguity and the activity dependence of β render the evaluation of γ pretty uncertain. Precision of β in classical studies was also low because of small data sizes. To undertake more detailed and large-scale data analysis as in [6, 40] is important.

Third, the interaction strength, which is assumed to be proportional to w_1w_2/r^β in the gravity model, may be nonlinear in weights. For example, use of $w_1^xw_2^x/r^\beta$ [26] results in $\gamma=1+a\beta/xd$. Real data actually support $0.73\le x\le 1.05$ [37], and x smaller than 1 increases γ to make it more realistic. By the same token, replacing $(w_1+w_2)/r^\beta$ with $(w_1+w_2)^x/r^\beta$ in the additive notation effectively changes β to β/x.

Next, let us relate our model to network search problems in which an agent on a vertex attempts to reach an unknown destination by traveling on edges. In small-world networks

defined by lattices supplied with long-range connections with density $g(r) \propto r^{-\delta}$, which are essentially equivalent to the random connection model [28], optimal search performance is realized when $\delta = d$ [20]. Even though the weighted gravity model is a different model, simple adoption of our formula suggests $d = \delta = a\beta$ and $\gamma = 1 + a\beta/d = 2$. Computer-related networks usually have $\gamma > 2$ presumably because they are growing. However, some social networks and peer-to-peer networks, which may be considered to be nongrowing, own γ close to 2 [2], enhancing the search ability.

Similarly, emergence of small-world networks in a geographical framework requires $d+1 > \delta > d$, while latticelike networks result from $\delta > d+1$, and $\delta < d$ induces randomlike networks with low clustering [18]. Simple-minded substitution of $\delta = a\beta$ leads to $d + 1 > a\beta > d$ and $2 < \gamma < 2 + d^{-1}$. Since we usually have $d = 2$ or 3, γ associated with general nongrowing small-world networks may be close to 2. To summarize, scale-free networks with γ around 2 may be optimal in the sense of the search performance and the small-world property. In addition, $\gamma = 2$ is the baseline scaling exponent of the nongeographical threshold graph [15], and it may also be the case for general cooperative nongrowing networks [10, 11, 12, 13, 14, 15, 17]. In contrast, $\gamma = 3$ is an important phase-transition point for percolation and dynamic epidemic processes [42]. The BA model has $\gamma = 3$, which may set the baseline γ for other competitive growing networks [2, 3, 4, 5, 6, 7, 8]. Our current speculation stems from the ansatz $\gamma = 1 + a\beta/d = 1 + \delta/d$ plugged into the results obtained from other models. Further investigation of this issue is an important future problem.

V. CONCLUSIONS

We have proposed and analyzed a geographical nongrowing network model based on thresholding the sum of two vertex weights. Our model contrasts with geographical growing models based on the BA model, and it naturally extends the threshold graph, the unit disk graph, and the gravity model, which are widely used in a range of fields. In proper regimes, small-world networks with scale-free degree distributions and the connection probability algebraically decaying in distance are generated, and they are consistent with many real data. In contrast to the nongeographical threshold model, what weight distribution is used matters for network properties. For scale-free networks to emerge, the weight should be distributed as specified by power laws. The weight distribution and the degree distribution

generally have different scaling exponents, and they are bridged by a relation involving the spatial dimension and the decay rate of the interaction strength.

Acknowledgments

We thank D. Harada for assistance in the numerical simulations in this work and S. Havlin and Y. Otake for helpful comments related to this work. This study is supported by RIKEN and a Grant-in-Aid for Young Scientists (B) (Grant No. 15700020) of Japan Society of the Promotion of Science.

---

[1] D. J. Watts and S. H. Strogatz, Nature (London) **393**, 440 (1998).

[2] A.-L. Barabási and R. Albert, Science **286**, 509 (1999); R. Albert and A.-L. Barabási, Rev. Mod. Phys. **74**, 47 (2002); S. N. Dorogovtsev and J. F. F. Mendes, Adv. Phys. **51**, 1079 (2002); M. E. J. Newman, SIAM Rev. **45**, 167 (2003).

[3] G. Bianconi and A.-L. Barabási, Phys. Rev. Lett. **86**, 5632 (2001).

[4] S. S. Manna and P. Sen, Phys. Rev. E **66**, 066114 (2002).

[5] R. Xulvi-Brunet and I. M. Sokolov, Phys. Rev. E **66**, 026118 (2002).

[6] S.-H. Yook, H. Jeong, and A.-L. Barabási, Proc. Natl. Acad. Sci. U.S.A. **99**, 13382 (2002).

[7] P. Sen and S. S. Manna, Phys. Rev. E **68**, 026104 (2003).

[8] E. Ravasz *et al.*, Science **297**, 1551 (2002); E. Ravasz and A.-L. Barabási, Phys. Rev. E **67**, 026112 (2003).

[9] A. Barrat, M. Barthélemy, and A. Vespignani, Phys. Rev. Lett. **92**, 228701 (2004); A. Barrat, M. Barthélemy, R. Pastor-Satorras, and A. Vespignani, Proc. Natl. Acad. Sci. U.S.A. **101**, 3747 (2004).

[10] G. Caldarelli, A. Capocci, P. De Los Rios, and M. A. Muñoz, Phys. Rev. Lett. **89**, 258702 (2002).

[11] K. -I. Goh, B. Kahng, and D. Kim, Phys. Rev. Lett. **87**, 278701 (2001); F. Chung and L. Lu, Proc. Natl. Acad. Sci. U.S.A. **99**, 15879 (2002); F. Chung, L. Lu, and V. Vu, *ibid.* **100**, 6313 (2003).

[12] Z. Toroczkai and K. E. Bassler, Nature (London) **428**, 716 (2004).

[13] M. Boguñá and R. Pastor-Satorras, Phys. Rev. E **68**, 036112 (2003).

[14] V. D. P. Servedio, G. Caldarelli, and P. Buttà, Phys. Rev. E **70**, 056126 (2004).

[15] N. Masuda, H. Miwa, and N. Konno, Phys. Rev. E. **70**, 036124 (2004).

[16] M. C. Golumbic, *Algorithmic Graph Theory and Perfect Graphs* (Academic Press, New York, 1980).

[17] A. F. Rozenfeld, R. Cohen, D. ben-Avraham, and S. Havlin, Phys. Rev. Lett. **89**, 218701 (2002).

[18] P. Sen, K. Banerjee, and T. Biswas, Phys. Rev. E **66**, 037102 (2002).

[19] M. Biskup, Ann. Prob. **32**, 2938 (2004).

[20] J. M. Kleinberg, Nature (London) **406**, 845 (2000); M. Franceschetti and R. Meester, Preprint (2004).

[21] B. M. Waxman, IEEE J. Sel. Areas Commun. **6**, 1617 (1988).

[22] S. Amari, Biol. Cybern. **27**, 77 (1977); M. Usher, M. Stemmler, C. Koch, and Z. Olami, Neural Comput. **6**, 795 (1994); A. Compte, N. Brunel, P. S. Goldman-Rakic, and X.-J. Wang, Cereb. Cortex **10**, 910 (2000); C. R. Laing *et al.*, SIAM J. Appl. Math. **63**, 62 (2002); C. Mehring *et al.*, Biol. Cybern. **88**, 395 (2003).

[23] B. Hellwig, Biol. Cybern. **82**, 111 (2000).

[24] V. M. Eguíluz *et al.*, Phys. Rev. Lett. **94**, 018102 (2005).

[25] J. Karbowski, Phys. Rev. Lett. **86**, 3674 (2001).

[26] K. E. Haynes and A. S. Fotheringham, *Gravity and Spatial Interaction Models* (SAGE Publications, Beverly Hills, CA, 1984).

[27] B. G. Hutchinson and D. P. Smith, Can. J. Civ. Eng. **6**, 308 (1979).

[28] R. Meester and R. Roy, *Continuum Percolation* (Cambridge University Press, Cambridge, 1996).

[29] B. N. Clark, C. J. Colbourn, and D. S. Johnson, Discrete Math. **86**, 165 (1990); A. V. Fishkin, Lect. Notes Comput. Sci. **2909**, 260 (2004).

[30] G. K. Zipf, Am. Sociol. Rev. **11**, 677 (1947).

[31] G. K. Zipf, *Human Behavior and the Principle of Least Effort* (Addison-Wesley, Cambridge, MA, 1949); M. Marsili and Y.-C. Zhang, Phys. Rev. Lett. **80**, 2741 (1997); D. H. Zanette and S. C. Manrubia, *ibid.* **79**, 523 (1998).

[32] K. T. Rosen and M. Resnick, J. Urban Econ. **8**, 165 (1980).

[33] R. L. Axtell, Science **293**, 1818 (2001).

[34] B. A. Huberman and L. A. Adamic, Nature (London) **401**, 131 (1999).

[35] T. Kaizoji, Physica A **326**, 256 (2003); C. Andersson *et al.*, Phys. Rev. E **68**, 036124 (2003).

[36] M. Levy and S. Solomon, Int. J. Mod. Phys. C **7**, 595 (1996); K. Okuyama, M. Takayasu, and H. Takayasu, Physica A **269**, 125 (1999).

[37] W. H. Long, Ann. Regional Sci. **4**, 97 (1970); E. P. Howrey, J. Regional Sci. **9**, 215 (1969).

[38] A. S. Fotheringham, Ann. Assoc. Am. Geographers **71**, 425 (1981).

[39] R. L. Morrill and F. R. Pitts, Ann. Assoc. Am. Geographers **57**, 401 (1967).

[40] B. Latané *et al.*, Personality Social Psych. Bull. **21**, 795 (1995).

[41] G. N. Watson, *A Treatise on the Theory of Bessel Functions*, 2nd ver. (Cambridge University Press, Cambridge, 1995).

[42] R. Cohen, K. Erez, D. ben-Avraham, and S. Havlin, Phys. Rev. Lett. **85**, 4626 (2000); R. Pastor-Satorras and A. Vespignani, *ibid.* **86**, 3200 (2001).

Figure captions

Figure 1: Network properties with $h(r) = r^{-\beta}$ and the exponential weight distribution with $\lambda = 1$ and $\langle k \rangle = 20$. Dependence of (a) L and (b) C on β for $n = 2000$ (thinnest lines), 4000, 6000, 8000, and 10000 (thickest lines) is presented. The relation between L and n is shown in the inset of (a), with upper lines corresponding to larger β. Also shown are numerically obtained $p(k)$ (crosses) and $C(k)$ (circles) with $n = 10000$ for (c) $\beta = 0.5$, (d) $\beta = 1.5$, and (e) $\beta = 2.5$.

Figure 2: Network properties for the gravity model with the Pareto weight distribution with $a = 1$, $w_0 = 1$, and $\langle k \rangle = 20$. Dependence of (a) L and (b) C on β is presented. Also shown are numerically obtained $p(k)$ (crosses), $C(k)$ (circles) with $n = 10000$, and the theoretical prediction $p(k) \propto k^{-1-a\beta/d}$ (lines) for (c) $\beta = 2$, (d) $\beta = 3$, and (e) $\beta = 4$.

Figure 3: Numerically obtained $g(r)$ (circles) and the prediction by Eq. (39) (lines) for the gravity model with (a) $\beta = 2$ and (b) $\beta = 3$. The other parameter values are the same as those used in Fig. 2.

Figure 4: An example of the weighted gravity model on a one-dimensional ring. We set $n = 100$, $\beta = 1$, and $\langle k \rangle = 6$. The Pareto weight distribution with $a = 1$ and $w_0 = 1$ is used.

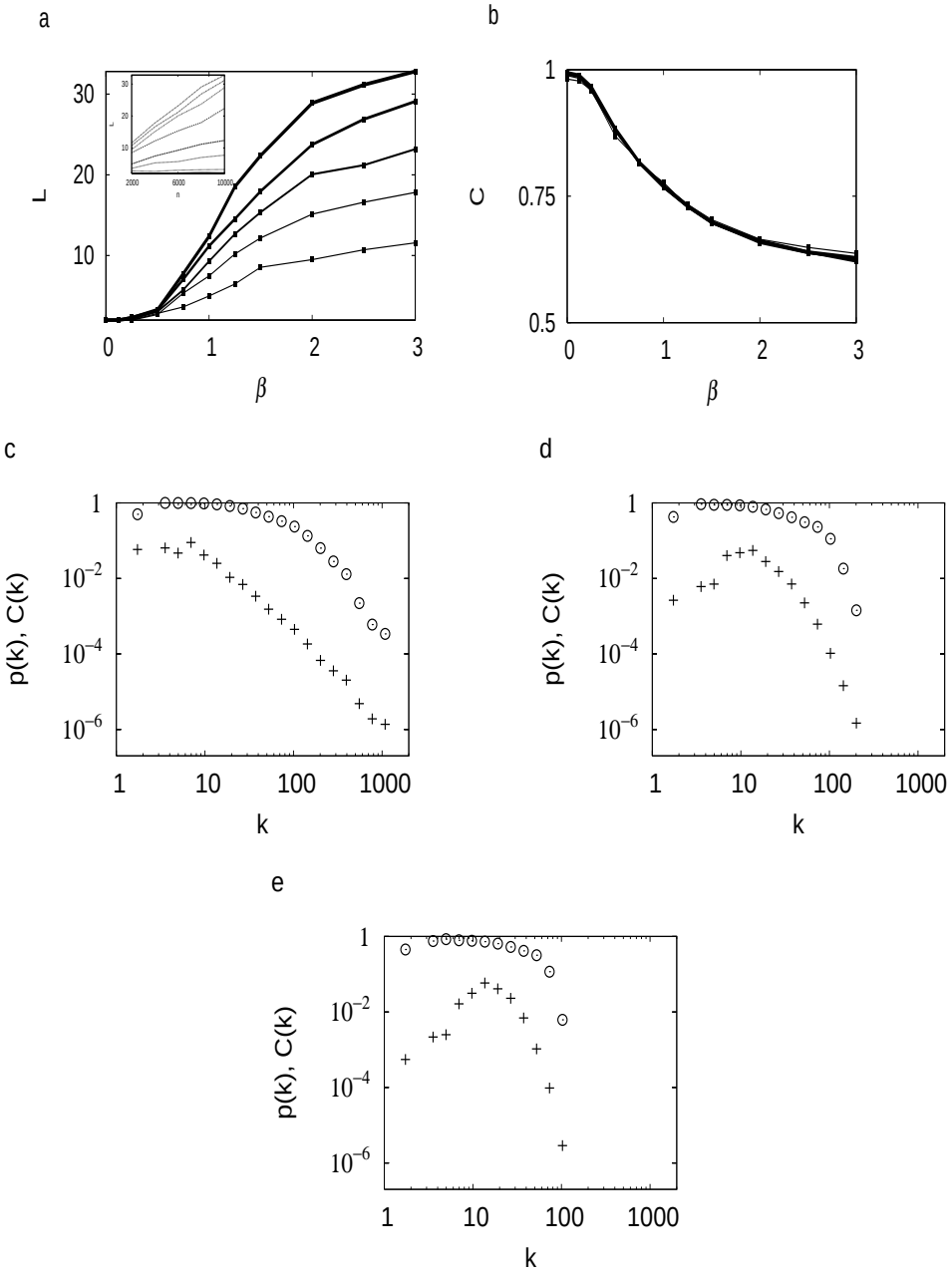

FIG. 1:

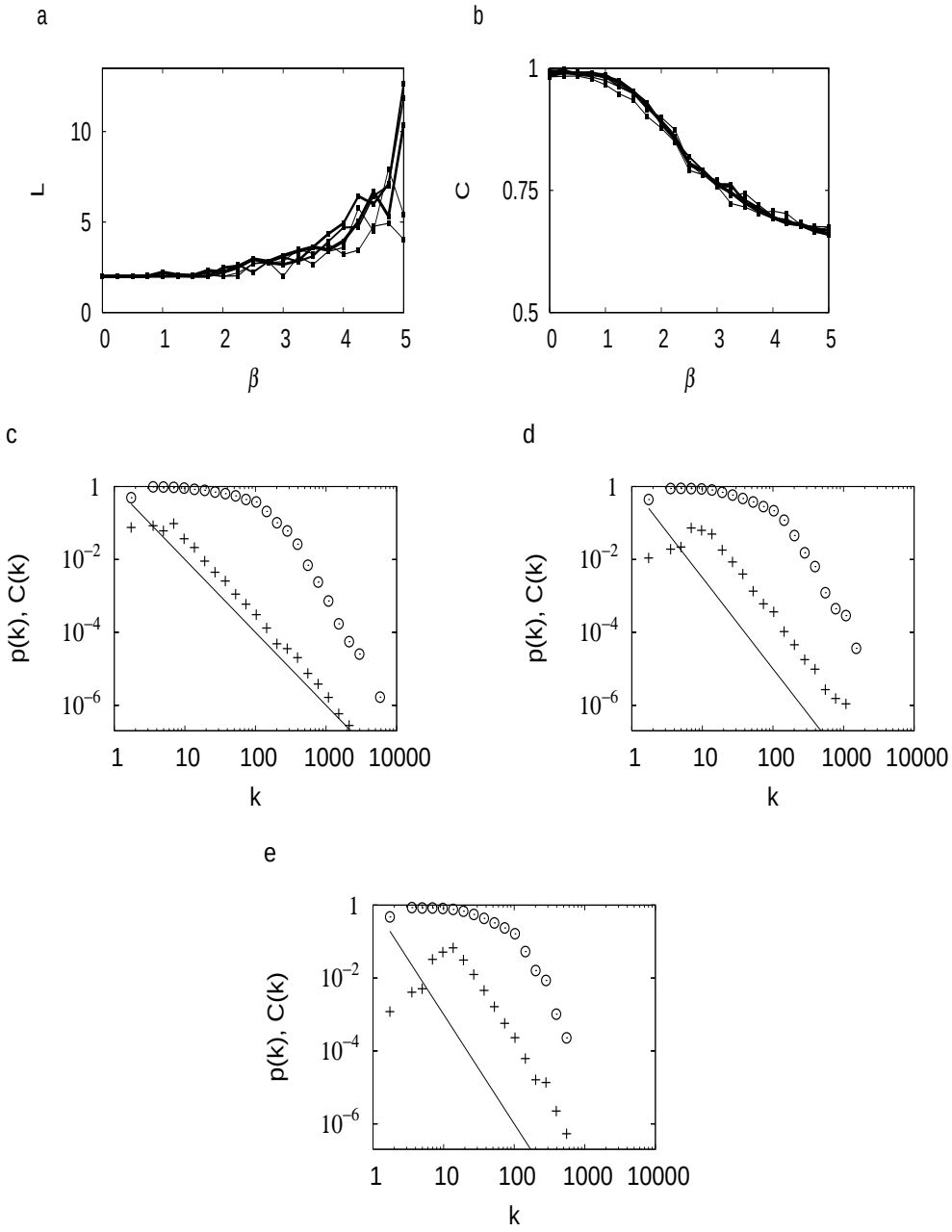

FIG. 2:

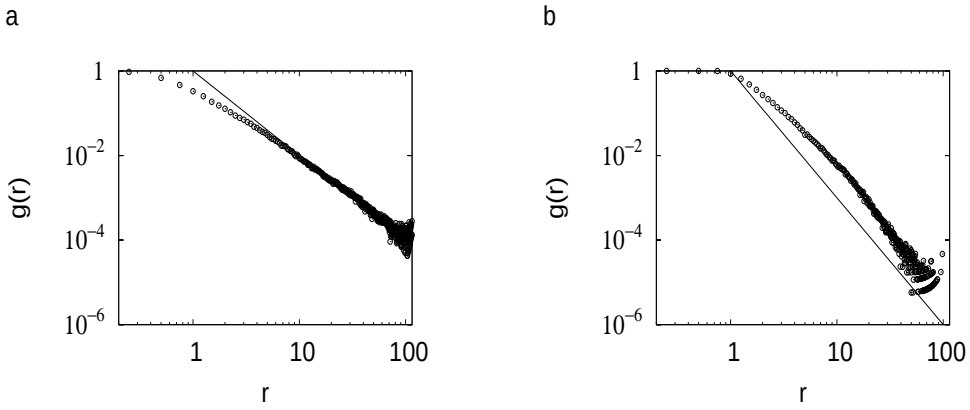

FIG. 3:

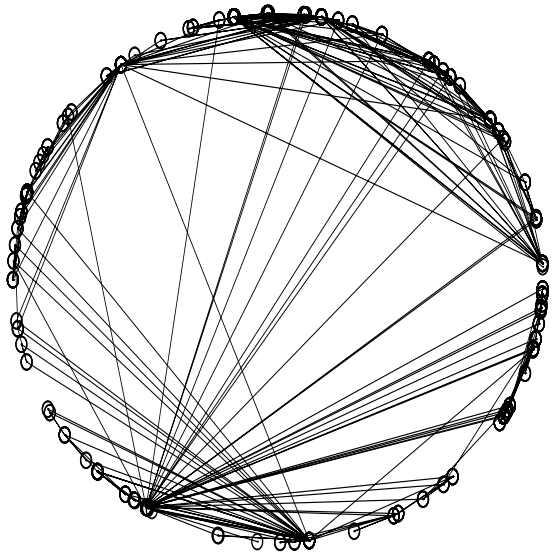

FIG. 4: